Tuning Space Mapping for Microwave Design Optimization

Slawomir Koziel [1], John W. Bandler [2] and Qingsha S. Cheng [2]

[1] Engineering Optimization & Modeling Center, School of Science and Engineering
Reykjavik University, 101 Reykjavik, Iceland
koziel@ru.is

[2] Simulation Optimization Systems Research Laboratory, Department of Electrical and Computer Engineering,
McMaster University, Hamilton, ON, Canada L8S 4K1
bandler@mcmaster.ca, chengq@mcmaster.ca

Abstract: Tuning space mapping (TSM) is one of the latest developments in simulation-driven microwave design optimization that combines space mapping with the concept of tuning, and exploits the co-calibrated port technology offered by Sonnet ***em***. TSM algorithms allow remarkably fast electromagnetics-based design optimization of microwave structures. In this paper, we review this technology and describe selected variants of TSM algorithms. Application examples are presented.

Keywords: Computer-aided design (CAD), Simulation-driven design, Tuning, Space mapping, Surrogate modeling, Electromagnetics-based design

1. Introduction

Space mapping (SM) is one of the most popular surrogate-based design optimization techniques in microwave engineering. It optimizes a CPU-intensive EM-simulated "fine" model through iterative optimization and updating of a suitable surrogate constructed from a so-called "coarse" model, a less accurate but cheaper to evaluate representation of the fine model (e.g., equivalent circuit) [1-3].

Tuning space mapping (TSM) [4], combines SM with the concept of tuning—widely used and understood in microwave engineering [5-6]. The surrogate model's role is taken by a tuning model, constructed by embedding circuit-theory based components into the fine model structure, and parameters of these circuit components are chosen to be tunable. The tuning model is updated and optimized with respect to appropriate tuning parameters. The optimal tuning values are translated into a modification of the fine model.

Several versions of the TSM algorithm have been proposed. In [7], an early version of TSM has been introduced (also referred to as the "Type 0" embedding [8]), in which the calibration generally involves an auxiliary model, typically a fast SM surrogate [7]. This version of embedding introduces minimal disturbance to the EM model so that the tuning model becomes a very accurate representation of the fine model. However, it has limited tuning capacity and suffers from difficulties in handling certain cross-sectional parameters [8]. Also, the calibration process is rather complicated.

TSM with embedded tuning components (ETSM) (so-called "Type 1" embedding) [8] addresses the drawbacks of the Type 0 embedding by replacing entire sections of the structure of interest by tuning elements. This allows easy tuning of cross-sectional parameters and simplifies the calibration process. However, ETSM requires more co-calibrated ports than TSM, which increases the EM simulation cost. And, typically, the ETSM requires more iterations to find a satisfactory design.

In [9], the fast version of ETSM (FETSM) is introduced, maintaining all the merits of ETSM while being substantially faster. In FETSM, the simulation of the structure with all co-calibrated ports is replaced by a simulation of the reduced structure where all designable sections are removed [9].

In this paper, we briefly review the art of tuning space mapping, describe the details of TSM, ETSM and FETSM, and present some illustration examples.

2. Tuning Space Mapping. TSM with Type-0 Embedding

A. Tuning Space Mapping Concept

We are concerned with the optimization problem

$$\boldsymbol{x}_f^* = \arg\min_{\boldsymbol{x}} U\left(\boldsymbol{R}_f(\boldsymbol{x})\right), \tag{1}$$

where $\boldsymbol{R}_f \in R^m$ is the response vector of a fine model of a device of interest, U is a merit function (e.g., a minimax function), $\boldsymbol{x}$ is a vector of design parameters, and $\boldsymbol{x}_f^*$ is the optimal solution to be determined.

Type-0 TSM exploits a tuning model $\boldsymbol{R}_t$ that contains relevant fine model data (e.g., *S*-parameters) at the current design, and tuning parameters (of the circuit elements inserted into the tuning ports). The tunable parameters are adjusted so that $\boldsymbol{R}_t$ satisfies the design specifications. The second model, $\boldsymbol{R}_c$, is used for calibration: it allows us to translate changes in the tuning parameters into relevant changes of the actual design variables; $\boldsymbol{R}_c$ depends on design parameters, tuning parameters (the same tuning elements are embedded in $\boldsymbol{R}_c$ as used in $\boldsymbol{R}_t$), and SM parameters, adjusted using a parameter extraction process [1] in order to have the model $\boldsymbol{R}_c$ meet certain matching conditions [4]. The conceptual illustrations of $\boldsymbol{R}_f$, $\boldsymbol{R}_t$ and $\boldsymbol{R}_c$ are shown in Fig. 1.

B. TSM Algorithm [7]

The TSM algorithm produces a sequence of designs $\boldsymbol{x}^{(i)}$, $i = 0, 1, \ldots$. The iteration of the algorithm consists of two steps: optimization of $\boldsymbol{R}_t$ and a calibration procedure. First, the current tuning model $\boldsymbol{R}_t^{(i)}$ is built using fine model data at point $\boldsymbol{x}^{(i)}$. In general, because the fine model has undergone a disturbance, the tuning model response may not agree with the response of the fine model at $\boldsymbol{x}^{(i)}$ even when the values of the tuning parameters $\boldsymbol{x}_t$ are set to zero, so these values must be adjusted to, say, $\boldsymbol{x}_{t.0}^{(i)}$ to obtain alignment:

$$\boldsymbol{x}_{t.0}^{(i)} = \arg\min_{\boldsymbol{x}_t} \left\| \boldsymbol{R}_f(\boldsymbol{x}^{(i)}) - \boldsymbol{R}_t^{(i)}(\boldsymbol{x}_t) \right\|. \tag{2}$$

In the next step, we optimize $\boldsymbol{R}_t^{(i)}$. The optimal values of the tuning parameters $\boldsymbol{x}_{t.1}^{(i)}$ as follows:

$$\boldsymbol{x}_{t.1}^{(i)} = \arg\min_{\boldsymbol{x}_t} U\left(\boldsymbol{R}_t^{(i)}(\boldsymbol{x}_t)\right). \tag{3}$$

Having $\boldsymbol{x}_{t.1}^{(i)}$ we perform the calibration procedure to determine changes in the design variables that yield the same change in the calibration model response as caused by $\boldsymbol{x}_{t.1}^{(i)} - \boldsymbol{x}_{t.0}^{(i)}$. We first adjust the SM parameters $\boldsymbol{p}^{(i)}$ of the calibration model to obtain a match with the fine model response at $\boldsymbol{x}^{(i)}$:

$$\boldsymbol{p}^{(i)} = \arg\min_{\boldsymbol{p}} \left\| \boldsymbol{R}_f(\boldsymbol{x}^{(i)}) - \boldsymbol{R}_c(\boldsymbol{x}^{(i)}, \boldsymbol{p}, \boldsymbol{x}_{t.0}^{(i)}) \right\|. \tag{4}$$

$\boldsymbol{R}_c$ is then optimized with respect to the design variables in order to obtain the next iteration point $\boldsymbol{x}^{(i+1)}$

$$\boldsymbol{x}^{(i+1)} = \arg\min_{\boldsymbol{x}} \left\| \boldsymbol{R}_t^{(i)}(\boldsymbol{x}_{t.1}^{(i)}) - \boldsymbol{R}_c(\boldsymbol{x}, \boldsymbol{p}^{(i)}, \boldsymbol{x}_{t.0}^{(i)}) \right\|. \tag{5}$$

Note that we use $\boldsymbol{x}_{t.0}^{(i)}$ in (4), which corresponds to the state of the tuning model after performing the alignment procedure (2), and $\boldsymbol{x}_{t.1}^{(i)}$ in (5), which corresponds to the optimized tuning model (cf. (3)). Thus, (4) and (5) allow us to find changes in the design variable values $\boldsymbol{x}^{(i+1)} - \boldsymbol{x}^{(i)}$ necessary to compensate the effect of changing the tuning parameters from $\boldsymbol{x}_{t.0}^{(i)}$ to $\boldsymbol{x}_{t.1}^{(i)}$.

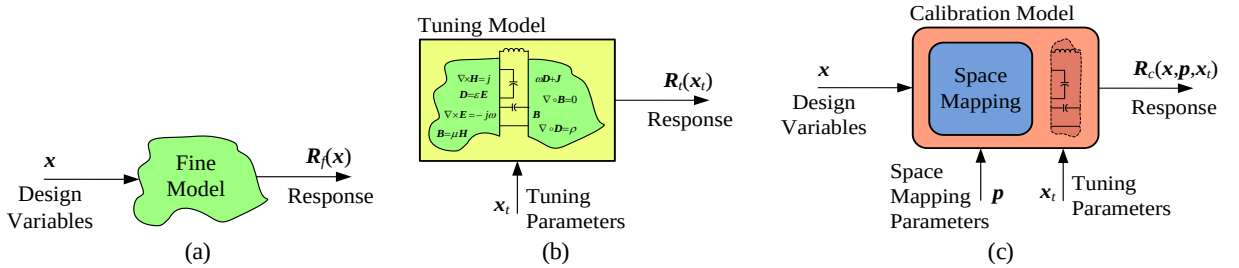

Fig. 1. Conceptual illustrations of the fine model, the tuning model and the calibration model [7]: (a) the fine model is typically based on a full-wave EM simulation, (b) the tuning model exploits the fine model "image" (e.g., in the form of *S*-parameters corresponding to the current design imported to the tuning model using suitable multiport data components) and a number of circuit-theory-based tuning elements, (c) the calibration model is usually an equivalent circuit dependent on the same design variables as $\boldsymbol{R}_f$, the same tuning parameters as $\boldsymbol{R}_t$ and a set of SM parameters used to align the calibration model with both $\boldsymbol{R}_f$ and $\boldsymbol{R}_t$ during the calibration process.

C. Design Example

Consider the box-section Chebyshev microstrip bandpass filter [10] (Fig. 2(a)). The design parameters are $\boldsymbol{x} = [L_1\ L_2\ L_3\ L_4\ L_5\ S_1\ S_2]^T$. The fine model is simulated in Sonnet ***em*** [11] with a grid of 1 mil × 2 mil. The design specifications are $|S_{21}| \le -20$ dB for 1.8 GHz $\le \omega \le$ 2.15 GHz and 2.65 GHz $\le \omega \le$ 3.0 GHz, and $|S_{21}| \ge -3$ dB for 2.4 GHz $\le \omega \le$ 2.5 GHz.

The tuning model is constructed by dividing the polygons corresponding to parameters L_1 to L_5 in the middle and inserting the tuning ports at the new cut edges. Its S28P data file is then loaded into the *S*-parameter component in Agilent ADS [12]. The circuit-theory coupled-line components and capacitor components are chosen to be the tuning elements and are inserted into each pair of tuning ports (Fig. 2(b)). The lengths of the imposed coupled-lines and the capacitances of the capacitors are assigned as the tuning parameters. The calibration model is an equivalent circuit that contains the same tuning elements as the tuning model [10] (Fig. 3). The initial design, $\boldsymbol{x}^{(0)} = [928\ 508\ 50\ 50\ 201\ 5\ 19]^T$ mil, is the optimal solution of the coarse model, i.e., the calibration model with zero values of the tuning parameters. Figure 4 shows the fine model response at the initial design, as well as the response after just one TSM iteration with $\boldsymbol{x}^{(1)} = [1022\ 398\ 46\ 56\ 235\ 4\ 10]^T$ mil (specification error –1.8 dB).

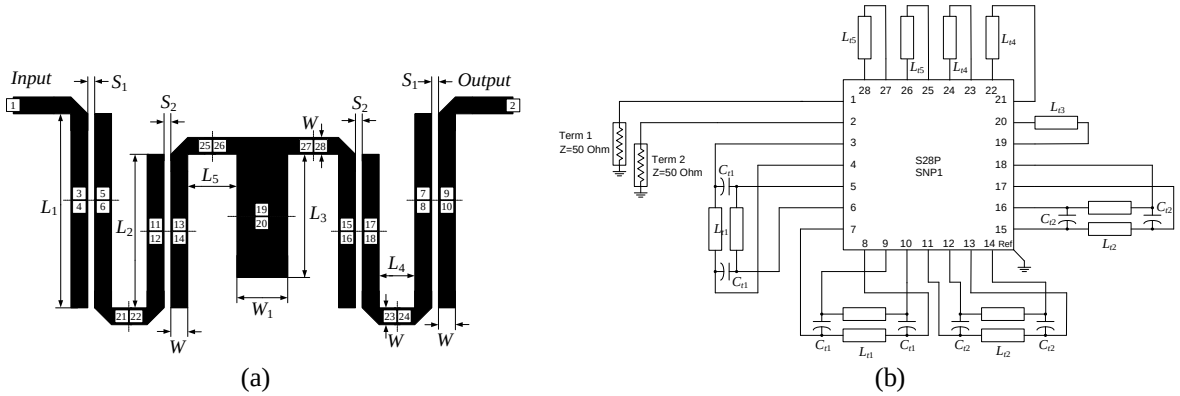

Fig. 2. Box-section Chebyshev bandpass filter: (a) geometry and places for inserting the tuning ports [10], (b) tuning model (Agilent ADS).

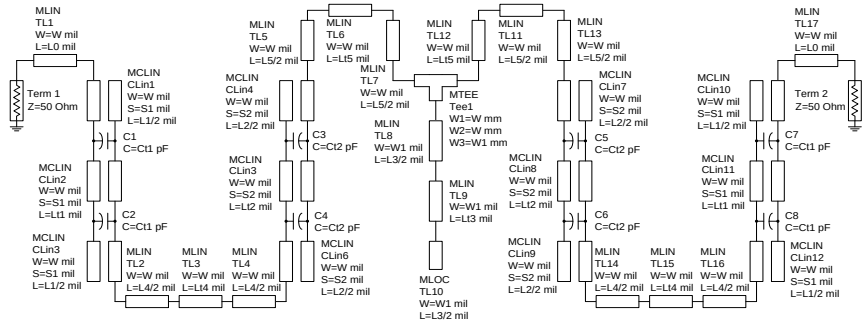

Fig. 3. Box-section Chebyshev bandpass filter: calibration model (Agilent ADS) [10].

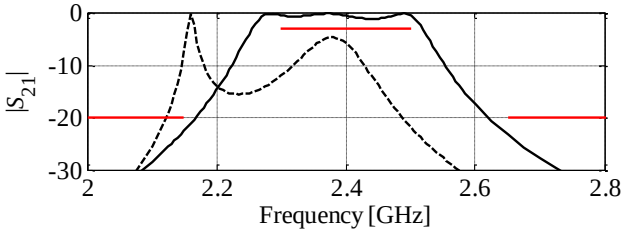

Fig. 4. Box-section Chebyshev bandpass filter: the fine model response at the initial design (dashed line) and at the design found after one iteration of the TSM algorithm (solid line).

3. TSM with Type-1 Embedding (ETSM)

A. ETSM Concept and Algorithm

TSM with embedded tuning elements (ETSM) involves the tuning model where certain designable sub-sections of the structure of interest are replaced with suitable tuning elements [8]. Preferably they are distributed circuit elements with physical dimensions corresponding to those of the fine model. After a simple alignment procedure, we match the tuning model with the fine model. Some of the fine-model couplings are preserved (or represented through *S*-parameters) in the tuning model. Next, the tuning model is optimized by changing the values of the design parameters of the embedded tuning elements to satisfy given design specifications. The obtained design parameters become our next fine model iterate. An example of inserting co-calibrated ports and replacing the coupled line segment by its circuit-theory model is illustrated in Fig. 5.

The iteration of ETSM consists of two steps: alignment of the tuning model with the fine model and the optimization of $\boldsymbol{R}_t$. First, based on fine model (with co-calibrated ports) data at the current design $\boldsymbol{x}^{(i)}$, the current tuning model $\boldsymbol{R}_t^{(i)}$ is built with appropriate tuning elements replacing certain $\boldsymbol{R}_f$ sections. The tuning model response may not agree with the response of the original fine model at $\boldsymbol{x}^{(i)}$. We align these models by:

$$\boldsymbol{p}^{(i)} = \arg\min_{\boldsymbol{p}} \left\| \boldsymbol{R}_f(\boldsymbol{x}^{(i)}) - \boldsymbol{R}_t^{(i)}(\boldsymbol{x}^{(i)}, \boldsymbol{p}) \right\|, \tag{6}$$

where $\boldsymbol{p}$ represents parameters of the tuning model used in the alignment process. These might be any parameters traditionally used by input, implicit or frequency SM [1]. In the next step, we optimize $\boldsymbol{R}_t^{(i)}$ to have it meet the design specifications. We obtain the next prediction of the design parameters $\boldsymbol{x}^{(i+1)}$ as:

$$\boldsymbol{x}^{(i+1)} = \arg\min_{\boldsymbol{x}} U\left(\boldsymbol{R}_t^{(i)}(\boldsymbol{x}, \boldsymbol{p}^{(i)})\right). \tag{7}$$

B. Fast ETSM (FETSM) [9]

Although the ETSM algorithm requires very few (typically 2 to 4) iterations to yield a satisfactory design, the simulation time of the structure containing co-calibrated ports is substantially longer than that of the original structure (without co-calibrated ports). For medium-scale problems (several design variables), the number of ports is 30, 50 or more, which increases the simulation time by at least one order of magnitude. As a result, the optimization cost expressed in the number of evaluations of the original structure is quite significant. Moreover, the EM simulation of the structure with co-calibrated ports is normally performed in each iteration of the ETSM algorithm.

In [9], a fast version of the ETSM algorithm (FETSM) is proposed. Instead of simulating the entire structure (with co-calibrated ports), we simulate the reduced structure with all the designable sub-sections removed beforehand. An example of such a procedure, corresponding to what is shown in Fig. 5, is explained in Fig. 6.

Fig. 5. Illustration of TSM with embedded tuning elements: (a) a coupled microstrip line of length *L*, (b) coupled line with co-calibrated ports inserted, (c) tuning model of the coupled line: middle section is replaced by the microstrip model (tuning element).

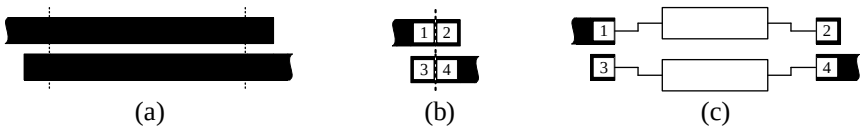

Fig. 6. Fast TSM with embedded tuning element: (a) a coupled microstrip line, (b) coupled line with co-calibrated ports and middle section removed, (c) tuning element inserted in between co-calibrated ports. The initial parameter values of the tuning element are chosen to coincide with those of the removed section. The number of co-calibrated ports is halved with respect to ETSM and the structure to be EM-simulated is simpler (no middle section).

From the tuning model point of view, the structure in Fig. 6(b) simulates the same fine-model couplings as the one in Fig. 5(b) because the middle section is being removed from the latter anyway. Thus, the accuracy of the tuning models based on both structures is expected to be similar. As the reduced structure is much simpler and the number of co-calibrated ports is half that of the entire structure, its simulation time is expected to be substantially smaller—comparable to the simulation time of the fine model (i.e., the original structure without ports). Moreover, because the reduced structure does not depend on the length parameters it is usually sufficient to perform its simulation once, at the first iteration of the FETSM algorithm.

C. Design Example

Consider the third-order Chebyshev bandpass filter [9] (Fig. 7(a)). The design parameters are $\boldsymbol{x} = [L_1\ L_2\ S_1\ S_2]^T$ mm. Other parameters are: $W_1 = W_2 = 0.4$ mm. The fine model is simulated in Sonnet ***em*** [11] with a grid of 0.1 mm × 0.01 mm. The design specifications are $|S_{21}| \geq -3$ dB for 1.8 GHz ≤ ω ≤ 2.2 GHz, and $|S_{21}| \leq -20$ dB for 1.0 GHz ≤ ω ≤ 1.6 GHz and 2.4 GHz ≤ ω ≤ 3.0 GHz. The evaluation time of the fine model is 27 minutes. The evaluation time of the fine model with the tuning ports is 11 hours.

For comparison purposes we consider both the ETSM and FETSM algorithms. The tuning model for the ETSM algorithm is shown in Fig. 7(b). In the case of the FETSM algorithm, the tuning model is constructed using the *S*-parameters of the reduced structure shown in Fig. 8(a) along with appropriate tuning elements, leading to the circuit of Fig. 8(b). Note that the reduced structure has a smaller number of co-calibrated ports (simulation time only 38 minutes).

Figure 9(a) shows the fine and tuning model responses at the initial design $\boldsymbol{x}^{(0)} = [14.6\ 15.3\ 0.56\ 0.53]^T$ mm. The misalignment between the models is reduced as in (6) using the additive perturbations of the design variables, dL_1, dL_2, dS_1, and dS_2, as the parameters $\boldsymbol{p}$. The tuning model response after performing (6) is also shown in Fig. 9(a). Figure 9(b) shows the fine model response after 2 iterations of the FETSM algorithm at $\boldsymbol{x}^{(2)} = [14.9\ 14.7\ 0.41\ 0.86]^T$ mm. The optimization results for ETSM and FETSM are summarized in Table 1. The quality of the final design is quite similar for both algorithms, which indicates that it is indeed sufficient to simulate the reduced structure to maintain the prediction capability of the tuning model. On the other hand, the computational cost is substantially lower for FETSM.

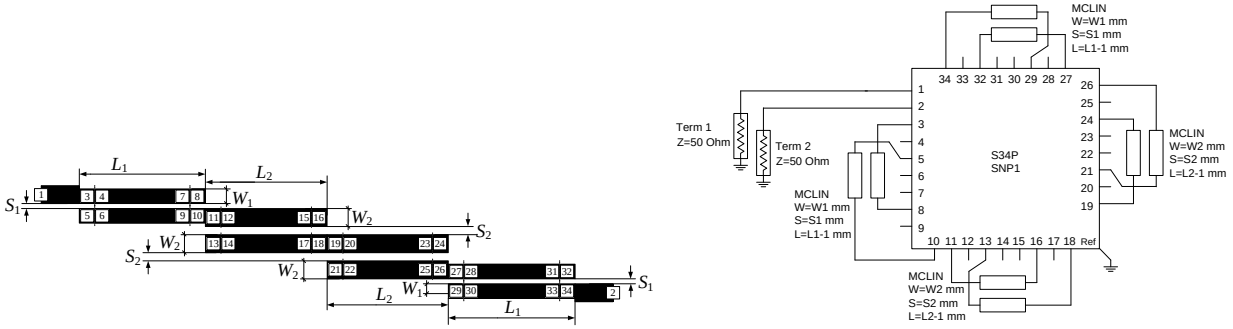

(a) (b)

Fig. 7. Third-order Chebyshev filter: (a) geometry and the places for inserting the tuning ports for ETSM algorithm [9], (b) tuning model for ETSM algorithm (Agilent ADS).

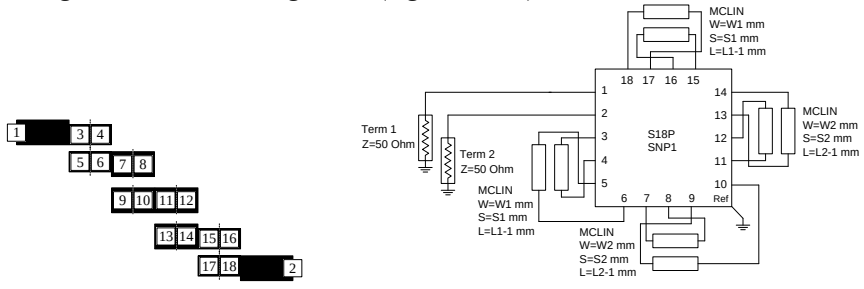

(a) (b)

Fig. 8. Third-order Chebyshev filter: (a) reduced structure and the places for inserting the tuning ports for FETSM algorithm, (b) tuning model for FETSM algorithm (Agilent ADS).

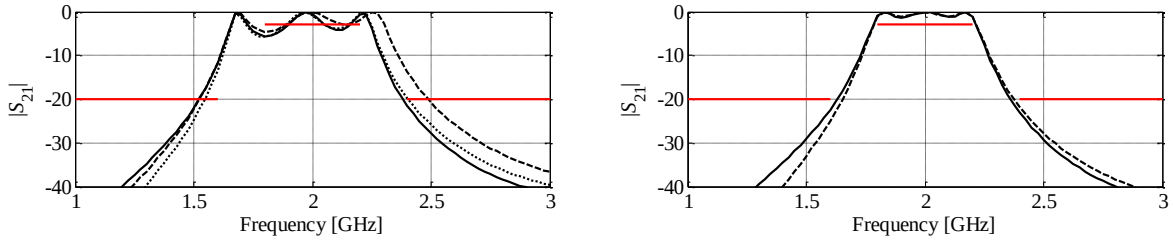

Fig. 9. Third-order Chebyshev filter optimized using FETSM: (a) responses at the initial design: fine model (solid line), tuning model (dashed lined), tuning model after the alignment procedure (2) (dotted line), (b) responses at the final design: the fine model (solid line) and the tuning model after the alignment procedure (dashed lined).

Table 1: Third-order Chebyshev filter: ETSM and FETSM optimization results

Algorithm	Optimization Results		Optimization Cost*	
	Number of Iterations	Specification Error	Total Time [hours]	Relative Cost (# of $\boldsymbol{R}_f$ evaluations)
ETSM	2	–1.7 dB	23.3	51.0
FETSM	2	–1.7 dB	1.5	3.4

* Excluding the fine model evaluation at the initial design.

4. Conclusion

We have reviewed tuning space mapping algorithms. Three variants of TSM have been discussed, including TSM with Type-0 and Type-1 embedding (ETSM), as well as a fast version of ETSM. Advantages and disadvantages of these techniques have been discussed along with illustrative examples.

Acknowledgement

The authors thank Sonnet Software, Inc., Syracuse, NY, making ***em***™ available. This work was supported in part by the Reykjavik University Development Fund under Grant T10006, by the Natural Sciences and Engineering Research Council of Canada under Grants RGPIN7239-06 and STPGP 381153-09, and by Bandler Corporation.

References

[1] J.W. Bandler, Q.S. Cheng, S.A. Dakroury, A.S. Mohamed, M.H. Bakr, K. Madsen, and J. Søndergaard, "Space mapping: the state of the art," *IEEE Trans. Microwave Theory Tech.*, vol. 52, no. 1, pp. 337-361, Jan. 2004.

[2] S. Koziel, Q.S. Cheng, and J.W. Bandler, "Space mapping," *IEEE Microwave Magazine*, vol. 9, no. 6, pp. 105-122, Dec. 2008.

[3] S. Amari, C. LeDrew, and W. Menzel, "Space-mapping optimization of planar coupled-resonator microwave filters," *IEEE Trans. Microwave Theory Tech.*, vol. 54, no. 5, pp. 2153-2159, May 2006.

[4] Q.S. Cheng, J.C. Rautio, J.W. Bandler, and S. Koziel, "Progress in simulator-based tuning—the art of tuning space mapping," *IEEE Microwave Magazine*, vol. 11, no. 4, pp. 96-110, Jun. 2010.

[5] J.C. Rautio, "RF design closure—companion modeling and tuning methods," *IEEE MTT IMS Workshop: Microwave Component Design using Space Mapping Technology*, San Francisco, CA, 2006.

[6] D.G. Swanson and R.J. Wenzel, "Fast analysis and optimization of combline filters using FEM," *IEEE MTT-S IMS Digest*, Boston, MA, pp. 1159-1162, July 2001.

[7] S. Koziel, J. Meng, J.W. Bandler, M.H. Bakr, and Q.S. Cheng, "Accelerated microwave design optimization with tuning space mapping," *IEEE Trans. Microwave Theory Tech.*, vol. 57, no. 2, pp. 383-394, Feb. 2009.

[8] Q.S. Cheng, J.W. Bandler, and S. Koziel, "Space mapping design framework exploiting tuning elements," *IEEE Trans. Microwave Theory Tech.*, vol. 58, no. 1, pp. 136-144, Jan. 2010.

[9] S. Koziel, J.W. Bandler, and Q.S. Cheng, "Design optimization of microwave circuits through fast embedded tuning space mapping," *Proc. 40th European Microwave Conference*, Paris, France, pp. 1186-1189, Sept./Oct. 2010.

[10] S. Koziel and J.W. Bandler, "Automated tuning space mapping implementation for rapid design optimization of microwave structures," *Int. Review of Progress in Applied Computational Electromagnetics, ACES 2009*, Monterey, CA, pp. 138-143, Mar., 2009.

[11] ***em***™ Version 12.54, Sonnet Software, Inc., 100 Elwood Davis Road, North Syracuse, NY 13212, USA, 2010.

[12] Agilent ADS, Version 2008, Agilent Technologies, 1400 Fountaingrove Parkway, Santa Rosa, CA 95403-1799, 2008.